Available online at www.sciencedirect.com
SCIENCE DIRECT®
Journal of Computational Physics 188 (2003) 139–156
JOURNAL OF COMPUTATIONAL PHYSICS
www.elsevier.com/locate/jcp

A Hybrid Symbolic Monte-Carlo method for radiative transfer equations

J.-F. Clouët, G. Samba *

Commissariat à l'Energie Atomique, BP 12, 91680 Bruyères Le Châtel, France

Received 11 July 2002; received in revised form 4 February 2003; accepted 2 March 2003

Abstract

We introduce a new model for radiative transfer equations where low energy groups are treated in the diffusion approximation whereas high energy groups are solution of the classical transport equation. This enables to extend the range of validity of usual Implicit Monte-Carlo techniques which behave poorly in regions characterized by a small mean free path. We show that Fleck's numerical scheme [J. Comput. Phys. 8 (1971) 313] is not adapted to this modeling and we present an application of Symbolic Monte-Carlo. Properties of the Monte-Carlo matrix are discussed and numerical results are presented.

AMS: 65C05; 85A25

Keywords: Monte-Carlo method; Radiative transfer

1. Introduction

When matter is brought to very high temperature, energy transported by radiation cannot be neglected. It is then necessary, when describing fluid motion, to take into account the exchange of energy between matter and a photon gas propagating at the speed of light: these are the radiation hydrodynamics equation [9]. In simplest models, photons are supposed to be at local thermodynamic equilibrium: their distribution function is a Planck's function taken at the temperature of matter. In the most general cases equilibrium hypothesis must be removed and the equation describing time evolution of the distribution of photons is an integro-differential transport equation strongly coupled to the matter energy equation. In the absence of fluid motion and neglecting Compton scattering and considering matter in local thermodynamical equilibrium, it writes as

* Corresponding author.
E-mail addresses: jean-francois.clouet@cea.fr (J.-F. Clouët), gerald.samba@cea.fr (G. Samba).

0021-9991/03/$ - see front matter
doi:10.1016/S0021-9991(03)00158-X

$$\begin{aligned} &\partial_t I_\nu + c\vec{\Omega}\cdot\nabla I_\nu + c\sigma_\nu\left(I_\nu - \frac{B_\nu(T)}{4\pi}\right) = 0,\\ &\partial_t E(T) + \int\int \sigma_\nu\left(\frac{B_\nu(T)}{4\pi} - I_\nu\right)\mathrm{d}\nu\,\mathrm{d}\vec{\Omega} = 0, \end{aligned} \tag{1}$$

where radiative intensity I_ν depends on frequency ν, direction $\vec{\Omega}$, space position x and time t. c is the speed of light, σ_ν the emission–absorption opacity, T is the matter temperature, $E(T)$ is the internal energy and the Planck's function $B_\nu(T)$ is given by

$$B_\nu(T) = \frac{2h\nu^3}{c^2}\frac{1}{\exp(h\nu/kT)-1}.$$

Despite the rapid progress of deterministic algorithms (see [1] for a recent contribution), Monte-Carlo methods are still very popular for solving radiative transfer equations. This is especially the case for 2D and 3D problems because the number of unknowns becomes rapidly prohibitive. Moreover, knowing exactly the full distribution function $I(\nu,\vec{\Omega},x,t)$ is often of little interest and we would prefer to compute accurately the absorbed energy, i.e., $\int\int \sigma_\nu I_\nu \mathrm{d}\nu\,\mathrm{d}\vec{\Omega}$: this can be seen as an integration on a three-dimensional space and Monte-Carlo methods are known to be competitive against deterministic methods for such problems.

On the other hand, whereas deterministic methods can be designed for treating at the same time regions with small and large mean free path, Monte-Carlo methods suffer from severe drawbacks when used in optically thick media because statistics usually become very poor. One of the solutions to overcome this difficulty is to introduce a hybrid formulation of radiative transport equations and to solve a diffusion equation where diffusion approximation is valid (see [5] for a recent review). One of the issues we have to address if we want to use this approach is the location of the boundary between transport and diffusion formulations. First, it has to be changing in time when temperature evolves because the mean free path is usually an increasing function of temperature: some material which is initially optically thick can become optically thin. Moreover, when using a spectral discretization a new problem appears: because mean free path is also usually an increasing function of frequency, low frequencies must be treated in the diffusion approximation whereas high frequency photons are far from equilibrium and require a transport description.

The purpose of this paper is to present a new hybrid formulation of radiative transfer equations based on the following idea: given some criterion on the mean free path, we can divide the population of photons at a given position into two families (one equilibrium family and one out of equilibrium) and solve for each family either a diffusion equation or a transport equation. This will enable to obtain automatically the diffusion limit seeked by deterministic methods provided that the given criterion has some physical content and to keep the advantages of Monte-Carlo methods with respect to computational cost.

The paper is organized as follows: in the next section, we introduce the notion of spectral cut-off and the new modeling of the transfer equations. In Section 3, we describe the numerical scheme based on symbolic Monte-Carlo method. In particular, we will make precise the numerical implementation of the generalized Marshak condition that arises at the interface between two regions whose cutting frequencies are different. In Section 4, we prove that the linear system constructed during the Monte-Carlo step is invertible. At last, we will present an application to a test case described in [8] which consists in computing the propagation of a Marshak wave with two energy groups, one optically thick and one optically thin and we conclude by discussing some computational issues.

2. Modeling

In order to numerically solve Eqs. (1), we introduce a spectral discretization. We define K energy groups (ν_k,ν_{k+1}) and the variables

$$I_k = \int_{\nu_k}^{\nu_{k+1}} I_\nu \,\mathrm{d}\nu, \quad B_\nu(T) = \int_{\nu_k}^{\nu_{k+1}} B_\nu(T)\,\mathrm{d}\nu.$$

Throughout the paper, we shall use only the Planck mean for opacities

$$\sigma_k(T) = \int_{\nu_k}^{\nu_{k+1}} \sigma_\nu(T) B_\nu(T)\,\mathrm{d}\nu \Big/ \int_{\nu_k}^{\nu_{k+1}} B_\nu(T)\,\mathrm{d}\nu.$$

We shall also denote by b_k the reduced Planck's function $b_k(T) = B_k(T)/(aT^4)$. Because all of the features of the model are already there in the linear case, for the sake of simplicity, we shall assume that b_k and σ_k do not depend of temperature and that the equation of state is linear with respect to $\Theta_M = aT^4$. Taking into account the non-linearities leads to the use of standard Newton's techniques for handling non-linear equations but does not change our analysis. To simplify notations, we make a change of physical units so that speed of light c is set to 1 and $E(T) \equiv \Theta_M$. We thus obtain

$$\begin{aligned} &\partial_t I_k + \vec{\Omega}\cdot\nabla I_k + \sigma_k\left(I_k - \frac{b_k}{4\pi}\Theta_M\right) = 0, \\ &\partial_t \Theta_M + \sum_{k=1}^{K} \int \sigma_k\left(\frac{b_k}{4\pi}\Theta_M - I_k\right)\mathrm{d}\vec{\Omega} = 0, \end{aligned} \tag{2}$$

with appropriate boundary conditions and initial values.

It is well known (see [7]) that when mean free path is small in front of some typical length scale, then P1 approximation is valid and radiative intensity can be approximated as

$$I_k(\vec{\Omega}) = \frac{E_k}{4\pi} + \frac{3}{4\pi}\vec{\Omega}\cdot\vec{F}_k, \tag{3}$$

where radiative energy E_k and radiative flux $\vec{F}_k$ are the zeroth and first order moments of radiative intensity I_k and do not depend on direction of propagation $\vec{\Omega}$. Furthermore, when thermal equilibrium is achieved (i.e., when temperature is slowly varying over many mean free paths) one gets simple formulas for these quantities

$$E_k = b_k\Theta_M; \quad \vec{F}_k = -\frac{b_k}{3\sigma_k}\nabla\Theta_M.$$

In some cases, radiative intensity is a Planckian function at some other temperature than Θ_M: for example, in an optically thin medium illuminated by a black body. So, for the sake of generality, we shall assume that:

$$E_k = b_k\Theta_T; \quad \vec{F}_k = -\frac{b_k}{3\sigma_k}\nabla\Theta_T \tag{4}$$

with some temperature Θ_T which can differ from Θ_M. So a way to obtain the diffusion limit for (2) is to use approximation (3) and (4) when possible. This can depend on which energy group we are considering. As mean free path is usually a growing function of energy, approximation (3) and (4) can be valid for low energy groups and not for high energy groups.

These remarks lead us to the introduction of two auxiliary variables:

- $T_T(x,t)$ the thermalization temperature (we shall actually use $\Theta_T = aT_T^4$).
- $\nu_{k^c(x,t)}$ the spectral cut-off ($\nu_{k^c(x,t)}$ is one of the discrete frequencies $\{\nu_1,\ldots,\nu_K\}$ which define the spectral discretization).

These variables are such that:

$$\begin{aligned} &\text{for } k \leqslant k^{\mathrm{c}}(x,t), \quad I_k(\vec{\Omega}) = \frac{b_k}{4\pi}\Theta_T - \frac{b_k}{4\pi\sigma_k}\vec{\Omega}\cdot\nabla\Theta_T, \\ &\text{for } k > k^{\mathrm{c}}(x,t), \quad I_k(\vec{\Omega}) \text{ is solution of the transport equation.} \end{aligned} \tag{5}$$

In other words, for $k \leqslant k^{\mathrm{c}}(x,t)$, we consider that spectral distribution of radiation field is at equilibrium, i.e., it is represented by a Planck's function but at some thermalization temperature T_T which can differ from matter temperature. For $k > k^{\mathrm{c}}(x,t)$, photons are out of equilibrium and their distribution function is found by solving the transport equation. An example of such distribution is displayed in Fig. 1: the spectral cut-off is set to 3.5 (arbitrary units) with $\Theta_M > \Theta_T$. Of course, the assumption that I_k is Planckian for $k \leqslant k^{\mathrm{c}}$ is a strong assumption because it means that all groups of energy are coupled at low frequency. This is not the case for example in the multigroup diffusion model. We shall come back to this remark later on.

Let us assume for a while that $k^{\mathrm{c}}(x,t)$ does not depend on space and time. If we put approximation (5) into the transport equation and integrate with respect to angle, we get for $k \leqslant k^{\mathrm{c}}$

$$b_k\partial_t\Theta_T + \sigma_k b_k(\Theta_T - \Theta_M) = \int \vec{\Omega}\cdot\nabla\left(\frac{b_k}{4\pi\sigma_k}\vec{\Omega}\cdot\nabla\Theta_T\right) = \operatorname{div}\left(\frac{b_k}{3\sigma_k}\nabla\Theta_T\right).$$

Adding these k^{c} equalities we obtain the following diffusion equation for the thermalization temperature

$$\alpha\partial_t\Theta_T + \sigma^{\mathrm{E}}(\Theta_T - \Theta_M) = \operatorname{div}\left(\frac{1}{3\sigma^{\mathrm{D}}}\nabla\Theta_T\right), \tag{6}$$

with

$$\alpha = \sum_{k=1}^{k^{\mathrm{c}}} b_k, \quad \sigma^{\mathrm{E}} = \sum_{k=1}^{k^{\mathrm{c}}} \sigma_k b_k, \quad \frac{1}{\sigma^{\mathrm{D}}} = \sum_{k=1}^{k^{\mathrm{c}}} \frac{b_k}{\sigma_k}.$$

Let us introduce also the total absorption opacity $\sigma^{\mathrm{T}} = \sum_{k=1}^{K} \sigma_k b_k$.

For $k > k^{\mathrm{c}}$, I_k is solution of the transport equation

$$\partial_t I_k + \vec{\Omega}\cdot\nabla I_k + \sigma_k\left(I_k - \frac{b_k}{4\pi}\Theta_M\right) = 0 \tag{7}$$

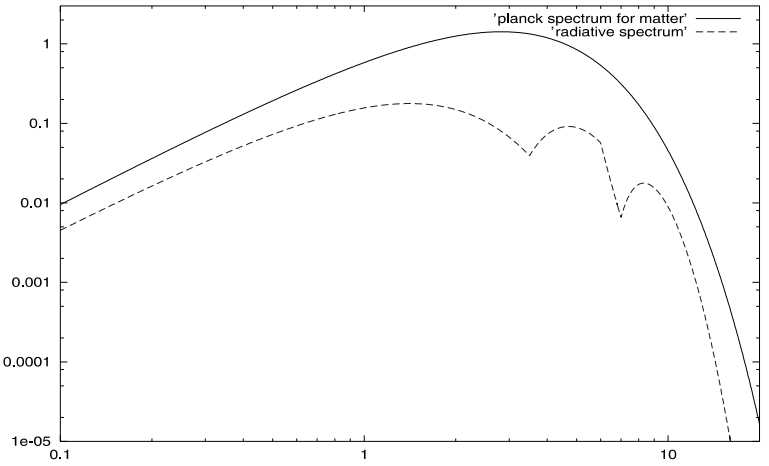

Fig. 1. Modeling of the spectrum as a function of frequency (arbitrary units).

and conservation of energy is written as

$$\partial_t \Theta_M + \sigma^{\mathrm{T}} \Theta_M - \sigma^{\mathrm{E}} \Theta_T - \sum_{k=k^{\mathrm{c}}+1}^{K} \sigma_k \int I_k(\vec{\Omega})\,\mathrm{d}\vec{\Omega} = 0. \tag{8}$$

Radiative energy is just defined by

$$aT_R^4 \equiv \Theta_R = \alpha \Theta_T + \sum_{k=k^{\mathrm{c}}+1}^{K} \int I_k(\vec{\Omega})\,\mathrm{d}\vec{\Omega}$$

and we can easily check that total energy $\Theta_R + \Theta_T$ is conserved.

Consider now the more general situation where $k^{\mathrm{c}}(x,t)$ depends on position x but not on time t. It means that we have transport–diffusion interfaces located at discontinuities of the discrete function $x \mapsto k^{\mathrm{c}}(x,t)$. The general situation is represented in Fig. 2. We must now describe the boundary conditions for system (6)–(8) at such an interface Γ. We denote by indices L and R the functions at the left and at the right side of interface Γ and $\vec{n}$ the vector normal to Γ oriented from left to right. We suppose that $k_{\mathrm{R}} > k_{\mathrm{L}}$ so there are fewer groups of energy at equilibrium on the left side. The continuity conditions are:

(i) For $k > k_{\mathrm{R}}$, we write continuity of radiative intensity

$$I_k(x,\vec{\Omega},t)_{|\Gamma^{\mathrm{L}}} = I_k(x,\vec{\Omega},t)_{|\Gamma^{\mathrm{R}}}. \tag{9}$$

(ii) For $k \leqslant k_{\mathrm{L}}$, we write continuity of net fluxes

$$\left(\frac{1}{\sigma^{\mathrm{D}}} \nabla \Theta_T\right)_{|\Gamma^{\mathrm{L}}} \cdot \vec{n} = \left(\frac{1}{\sigma^{\mathrm{D}}} \nabla \Theta_T\right)_{|\Gamma^{\mathrm{R}}} \cdot \vec{n} \tag{10}$$

with

$$\frac{1}{\sigma^{\mathrm{D}}_{\Gamma^{\mathrm{L}}}} = \sum_{k=1}^{k_{\mathrm{L}}} \frac{b_k}{\sigma^{\mathrm{L}}_k}, \quad \frac{1}{\sigma^{\mathrm{D}}_{\Gamma^{\mathrm{R}}}} = \sum_{k=1}^{k_{\mathrm{L}}} \frac{b_k}{\sigma^{\mathrm{R}}_k}.$$

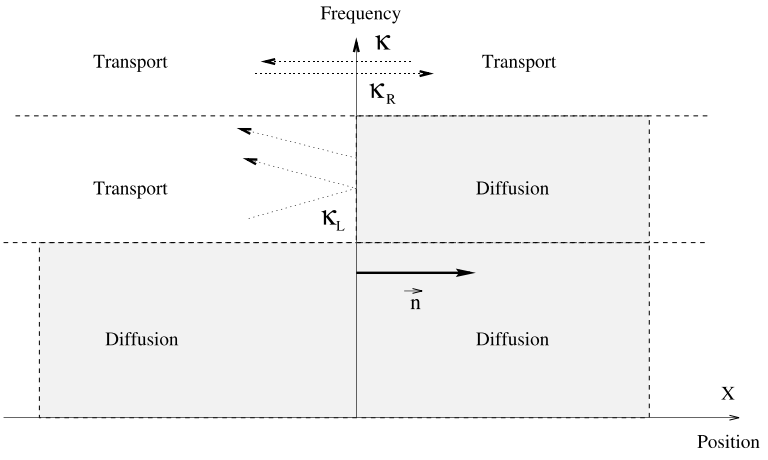

Fig. 2. Transport–diffusion interface.

(iii) For $k_{\mathrm{L}} < k \leqslant k_{\mathrm{R}}$ we use the Marshak condition (see [9])

$$\sum_{k=k_{\mathrm{L}}+1}^{k_{\mathrm{R}}} \int_{\vec{\Omega}\cdot\vec{n}>0} (\vec{\Omega}\cdot\vec{n}) \left(\frac{b_k}{4\pi}\Theta_T - \frac{b_k}{4\pi\sigma_k}\vec{\Omega}\cdot\nabla\Theta_T^{\mathrm{R}} \right)_{|\Gamma^{\mathrm{R}}} \mathrm{d}\vec{\Omega} = \sum_{k=k_{\mathrm{L}}+1}^{k_{\mathrm{R}}} \int_{\vec{\Omega}\cdot\vec{n}>0} (\vec{\Omega}\cdot\vec{n}) I_k(\vec{\Omega})_{|\Gamma^{\mathrm{L}}} \mathrm{d}\vec{\Omega}.$$

Integrating with respect to angles this writes as

$$\left(\frac{\alpha_\Gamma}{4}\Theta_T - \frac{1}{6\sigma_\Gamma^{\mathrm{I}}}\vec{n}\cdot\nabla\Theta_T \right)_{|\Gamma^{\mathrm{R}}} = \sum_{k=k_{\mathrm{L}}+1}^{k_{\mathrm{R}}} \int_{\vec{\Omega}\cdot\vec{n}>0} (\vec{\Omega}\cdot\vec{n}) I_k(\vec{\Omega})_{|\Gamma^{\mathrm{L}}} \mathrm{d}\vec{\Omega} \tag{11}$$

with

$$\alpha_\Gamma = \sum_{k=k_{\mathrm{L}}+1}^{k_{\mathrm{R}}} b_k, \quad \frac{1}{\sigma_\Gamma^{\mathrm{I}}} = \sum_{k=k_{\mathrm{L}}+1}^{k_{\mathrm{R}}} \frac{b_k}{\sigma_k^{\mathrm{R}}}. \tag{12}$$

We can now describe the behavior of the model as $k^{\mathrm{c}}(x,t)$ evolves in time: it is simply determined by the conservation of radiative energy. Suppose that at a given location x_0, the function $t \mapsto k^{\mathrm{c}}(x_0,t)$ has a discontinuity at time t_0 and denote by k^- and k^+ the values before and after t_0.

(i) If $k^+ > k^-$, some energy groups which were initially out of equilibrium achieve equilibrium at some new thermalization temperature Θ_T^+ given by

$$\left(\sum_{k=1}^{k^+} b_k \right) \Theta_T^+ = \left(\sum_{k=1}^{k^-} b_k \right) \Theta_T^- + \sum_{k=k^-+1}^{k^+} \int I_k(x_0,\vec{\Omega},t_0)\,\mathrm{d}\vec{\Omega}.$$

(ii) If $k^+ < k^-$, the thermalization temperature remains unchanged and the transport equation is solved for groups $k^+ + 1, \ldots, k^-$ with initial values

$$I_k(x_0,\vec{\Omega},t_0^+) = \frac{b_k}{4\pi}\Theta_T^- - \frac{b_k}{4\pi\sigma_k}\vec{\Omega}\cdot\nabla\Theta_T^-.$$

There are many ways to properly define the spectral cut-off $v_{k^{\mathrm{c}}(x,t)}$ such that P1 approximation (3) holds true. Of course some restrictions have to be imposed so that problem is well posed. In particular, for the transport–diffusion conditions it is necessary to define vectors $\vec{n}$ normal to surfaces $k^{\mathrm{c}}(x,t) = \text{constant}$: these interfaces must be at least piecewise C^1 surfaces. But apart from these "obvious" considerations, any local criteria based on the ratio between the spectral mean free path and some characteristic macroscopic length is a good candidate for defining $v_{k^{\mathrm{c}}(x,t)}$. We will give some examples in Section 5.

From a numerical point of view, we could consider the case where P1 approximation stands for some groups $k_1, \ldots, k_j$ which are not necessarily contiguous. Extension of discontinuity conditions is straightforward but we will not consider this case because there is no physical reason for which these groups of energy would be represented by a Planckian function at the *same* temperature. It would be preferable to use a hybrid method with transport equations coupled to a system of diffusion equations for each thermalized group instead of a single gray diffusion equation over a fraction of the whole spectrum.

3. Numerical scheme

The system which has to be solved numerically is composed of one diffusion equation (6), one transport equation (7) and one ordinary differential equation (8). These equations are coupled through terms on the right-hand side and through continuity conditions (9)–(11) which occur at the discontinuities of the function $k^c(x,t)$. Of course the most expensive step of the algorithm will consist in solving the transport equation and as said in Section 1, we want to restrict ourselves to Monte-Carlo method for this step. It is well known that implicit time discretization is necessary for solving radiative transfer when the matter and the photon gas are strongly coupled which is our case. So, we must choose an implicit Monte-Carlo method. There are two families of Monte-Carlo methods for radiative transfer equations:

1. Implicit Monte-Carlo (IMC) methods based on the seminal work of Fleck and Cumming [4]. These are predictor–corrector techniques: the energy equation provides a prediction of the temperature at the end of the time-step as a function of radiative intensity. Transport equation is then solved with this temperature as a source term. Finally, knowing the energy deposit, energy equation is exactly solved.
2. Symbolic Monte-Carlo (SMC) methods (see [2,6]) which consists in solving symbolically the transport equation, the source term being replaced by indicatrix functions, and then solve the energy balance equation (see below for further details).

It turns out that IMC is not well adapted for solving (6)–(8) and we would rather use SMC. The reason is the following. If we use the predictor–corrector technique then the source term that has to be used in the transport equation comes from integration of the energy balance equation over one time-step:

$$\tilde{\Theta}_M = a\Theta_M^0 + b\Theta_T + \sum_{k>k^c} \int c_k I_k(\vec{\Omega})\,\mathrm{d}\vec{\Omega},$$

where a, b and $(c_k)_{k>k^c}$ are some constants which only depend on opacity and time-step and Θ_M^0 is the value of the matter temperature at the beginning of the time-step. But it is not possible to use this prediction for the source term because it involves the solution Θ_T of diffusion equation (6) at the end of the time-step. It would then be necessary to get a prediction of Θ_T which is not easy because of diffusion operator. In order to have a local prediction, we can either treat the diffusion operator in an explicit way and obtain an estimate of the form

$$\tilde{\Theta}_M = a\Theta_M^0 + b_0\Theta_T^0 + b_1 \operatorname{div}\left(\frac{1}{3\sigma^D}\nabla\Theta_T^0\right) + \sum_{k>k^c} \int c_k I_k(\vec{\Omega})\,\mathrm{d}\vec{\Omega},$$

or neglect it and obtain an estimate of the form

$$\tilde{\Theta}_M = a\Theta_M^0 + b\Theta_T^0 + \sum_{k>k^c} \int c_k I_k(\vec{\Omega})\,\mathrm{d}\vec{\Omega}.$$

But neither of these choices can be justified in the general case so IMC is not a good candidate for solving the whole system. In the sequel, we shall show that it is much easier to use SMC.

In the next section, we recall the principles of SMC method applied to radiative transfer equations. Then we show how this applies to the system without transport–diffusion interfaces. At last, we describe the numerical scheme in the most general case where function $x \mapsto k^c(x,t)$ is discontinuous.

3.1. Principles of Symbolic Monte-Carlo method

We recall briefly the main feature of the method and we refer to [6] for further details. For this section only, we will only consider a gray model problem consisting in one single transport equation

$$\partial_t I + \vec{\Omega} \cdot \nabla I + \sigma I = \sigma \Phi, \quad I_{|t=0} = I^0 \tag{13}$$

coupled with the energy balance equation

$$\partial_t \Phi + \sigma \left(4\pi \Phi - \int I \, \mathrm{d}\vec{\Omega} \right) = 0, \quad \Phi_{|t=0} = \Phi^0.$$

As Eq. (13) is linear, we can write $I = I^{\exp} + I^{\mathrm{imp}}$ where functions $I^{\exp}$ and I^{imp} are solution of

$$\partial_t I^{\exp} + \vec{\Omega} \cdot \nabla I^{\exp} + \sigma I^{\exp} = 0, \quad I^{\exp}_{|t=0} = I^0,$$
$$\partial_t I^{\mathrm{imp}} + \vec{\Omega} \cdot \nabla I^{\mathrm{imp}} + \sigma I^{\mathrm{imp}} = \sigma \Phi, \quad I^{\mathrm{imp}}_{|t=0} = 0.$$

In the equation for $I^{\exp}$ the source term is explicit (it is zero) whereas it is implicit in the equation for I^{imp}. Introducing the semi-group of linear operators $T_t = \mathrm{e}^{-t(\vec{\Omega} \cdot \nabla + \sigma)}$, we have:

$$I^{\exp} = T_t I^0, \quad I^{\mathrm{imp}} = \int_0^t T_{t-s}(\sigma \Phi) \, \mathrm{d}s.$$

The key point is to notice that, after space discretization, the discrete version of these linear operators are matrices which can be estimated by a Monte-Carlo method. More precisely, let us denote by $\xi_i(x)$ the indicatrix function of some cell i such that $\Phi(x) = \sum_i \Phi_i \xi_i(x)$ and $\sigma(x) = \sum_i \sigma_i \xi_i(x)$ then we have $I^{\mathrm{imp}}(x, \vec{\Omega}, t) = \sum_i \Phi_i v_i(x, \vec{\Omega}, t)$ where function v_i is solution of the transport equation

$$\partial_t v_i + \vec{\Omega} \cdot \nabla v_i + \sigma v_i = \sigma_i \xi_i. \tag{14}$$

Using this formula in the energy balance equation one gets

$$\partial_t \Phi + 4\pi\sigma\Phi = \sigma \int \left(\sum_i \Phi_i v_i(\vec{\Omega}) + I^{\exp} \right) \mathrm{d}\vec{\Omega}.$$

using an implicit time discretization and integrating over a cell j of volume V_j and time interval $(t, t + \Delta t)$, we obtain

$$V_j(\Phi_j - \Phi_j^0) + 4\pi\Delta t \sigma_j \Phi_j V_j - \int_t^{t+\Delta t} \mathrm{d}s \int \mathrm{d}\vec{\Omega} \, \sigma_j \int_{V_j} \mathrm{d}x \left(\sum_i \Phi_i v_i(x, \vec{\Omega}, s) + I^{\exp}(x, \vec{\Omega}, s) \right) = 0,$$

which can be rewritten as

$$V_j(1 + 4\pi\Delta t \sigma_j)\Phi_j + \sum_i M_{j,i} \Phi_i = S_j \tag{15}$$

with

$$S_j = V_j \Phi_j^0 + \sigma_j \int_t^{t+\Delta t} \mathrm{d}s \int \mathrm{d}\vec{\Omega} \int_{V_j} \mathrm{d}x \, I^{\exp}(x, \vec{\Omega}, s),$$

$$M_{j,i} = \sigma_j \int_t^{t+\Delta t} \mathrm{d}s \int \mathrm{d}\vec{\Omega} \int_{V_j} \mathrm{d}x \, v_i(x, \vec{\Omega}, s).$$

So SMC method consists in solving transport equations for v_i (14) with source term an indicatrix function. We take a census of deposited energy and compute a matrix $\tilde{M}$ whose elements $\tilde{M}_{j,i}$ have $M_{i,j}$ as mathe-

matical expectation. In the sequel, we will use the same notation for $\tilde{M}$ and M which we call the Monte-Carlo matrix. The Monte-Carlo particles that are used for this computation are called symbolic particles because they sample an indicatrix function: we must keep their originating cell all through the tracking and their initial weight is just a factor of proportionality to the emission energy Φ. Other non-symbolic particles are also tracked which correspond to the initial value problem without source term for $I^{\exp}$. Second step of the method consists in solving the linear system (15).

3.2. Numerical scheme without transport–diffusion interfaces

We now come to the system of equations (6)–(8) and we first consider the case where $k^{c}(x,t)$ is a constant function. For sake of simplicity, we will study the space discretization on a 1D regular mesh with cell size denoted by h because the choice for the spatial scheme for the diffusion operator is not an issue (we simply take a finite difference approximation of second order derivatives). For more complicated geometries (e.g., distorted multidimensional meshes) the situation is different.

We integrate Eqs. (6) and (8) over time-step $(t, t+\Delta t)$. Denoting with indices 0 values of the unknowns at the beginning of the time-step and using implicit time discretization, we get

$$\begin{aligned}
&\alpha(\Theta_T - \Theta_T^0) + \Delta t\sigma^{E}(\Theta_T - \Theta_M) = \Delta t \operatorname{div}\left(\frac{1}{3\sigma^{D}}\nabla\Theta_T\right),\\
&\Theta_M - \Theta_M^0 + \Delta t\sigma^{T}\Theta_M = \Delta t\sigma^{E}\Theta_T + \int_t^{t+\Delta t} \mathrm{d}s \sum_{k=k^{c}+1}^{K} \sigma_k \int I_k(\vec{\Omega})\,\mathrm{d}\vec{\Omega}.
\end{aligned} \tag{16}$$

Let us introduce now spatial discretization: Θ_M and Θ_T become vectors of size n and the SMC method enables us to compute an $n \times n$ matrix $\mathscr{M}$ such that

$$\int_t^{t+\Delta t} \mathrm{d}s \sum_{k=k^{c}+1}^{K} \sigma_k \int I_k(\vec{\Omega})\,\mathrm{d}\vec{\Omega} = S + \mathscr{M}\Theta_M. \tag{17}$$

On the other hand, using finite differences for the diffusion operator leads to the following approximation:

$$\Delta t \operatorname{div}\left(\frac{1}{3\sigma^{D}}\nabla\Theta_T\right) = \mathscr{D}\Theta_T, \tag{18}$$

where $\mathscr{D}$ is a tridiagonal matrix (we impose symmetric boundary conditions). Putting together (16)–(18) and denoting by I_d the $n \times n$ identity matrix we obtain, in matrix form

$$\mathscr{A}\begin{bmatrix}\Theta_T\\ \Theta_M\end{bmatrix} = \begin{bmatrix}\alpha\Theta_T^0\\ \Theta_M^0 + S\end{bmatrix}, \tag{19}$$

where the $2n \times 2n$ Monte-Carlo matrix $\mathscr{A}$ is just

$$\mathscr{A} = \begin{bmatrix}(\alpha + \Delta t\sigma^{E})I_d - \mathscr{D} & -\Delta t\sigma^{E} I_d\\ -\Delta t\sigma^{E} I_d & (1 + \Delta t\sigma^{T})I_d - \mathscr{M}\end{bmatrix}. \tag{20}$$

3.3. Numerical scheme with transport–diffusion interfaces

We now describe the modifications to this scheme when there is a discontinuity in the function $k^{c}(x,t)$. Using time discretization, $k^{c}(x,t)$ is computed at the beginning of the time-step. As explained in the previous section, we take into account the change in time of $k^{c}(x,t)$ by using conservation of energy:

(i) If $k^+ < k^-$, Monte-Carlo particles are created whose weight is just the change of energy $(\sum_{k=k^++1}^{k^-} b_k)\Theta_T^0$.
(ii) If $k^+ > k^-$, Monte-Carlo particles whose energy group is in the interval $(k^- + 1, k^+)$ are killed. The sum of their weights represents some energy E which is reintroduced in the thermalized part by solving the equation

$$\left(\sum_{k=1}^{k^+} b_k\right)\Theta_T^+ = \left(\sum_{k=1}^{k^-} b_k\right)\Theta_T^- + E.$$

We shall now discretize the boundary conditions at an interface Γ where $k^c(x,t)$ is discontinuous. Using space discretization Γ is now the interface between two cells L and R (we use the same notations as in Fig. 2).

(i) For $k > k_R$, continuity of radiative intensity is a direct consequence of the tracking of Monte-Carlo particles whose energy group is higher than k_T through Γ.
(ii) For $k \leqslant k_L$, we discretize the continuity of fluxes (10)

$$F_L = \frac{\Theta_T^\Gamma - \Theta_T^L}{\sigma_{T^L}^D h} = \frac{\Theta_T^R - \Theta_T^\Gamma}{\sigma_{T^R}^D h} = F_R. \tag{21}$$

We can eliminate the temperature at the interface Θ_T^Γ in (21) and we get

$$F_L = F_R = \frac{\Theta_T^R - \Theta_T^L}{\left(\sigma_{T^L}^D + \sigma_{T^R}^D\right)h}. \tag{22}$$

(iii) For $k_L < k \leqslant k_R$, we use Brockway's discretization of Marshak condition (11) (see [10]) which writes in our case

$$\begin{aligned} \sum_{k=k_L+1}^{k_R} (F_k^+ + F_k^-) &= \frac{\alpha_\Gamma}{2}\Theta_T^\Gamma, \\ \sum_{k=k_L+1}^{k_R} (F_k^+ - F_k^-) &= \frac{\Theta_T^R - \Theta_T^\Gamma}{3\sigma_\Gamma^I h}, \end{aligned} \tag{23}$$

where α_Γ and σ_Γ^I have been defined in (12) and F_k^- and F_k^+ are the fluxes entering and leaving the left cell at interface Γ.

After simple algebraic manipulations, we can eliminate in (23) the temperature at the interface Θ_T^Γ and obtain a relation between fluxes and temperature in the right diffusion cell Θ_T^R:

$$\sum_{k=k_L+1}^{k_R} F_k^+ = (1-\zeta)\sum_{k=k_L+1}^{k_R} F_k^- + \frac{\zeta\alpha_\Gamma}{4}\Theta_T^R, \tag{24}$$

with

$$\zeta = \frac{4}{3\sigma_\Gamma^I h\alpha_\Gamma + 2}.$$

We recover the expression given in [10] when $\alpha_\Gamma = 1$ which corresponds to the case of the "full" transport–diffusion interface $k_L = 0$ and $k_R = K$.

Relation (24) must be interpreted in terms of events for the tracking of Monte-Carlo particles. The term $(1-\zeta)\sum_{k=k_{\mathrm{L}}+1}^{k_{\mathrm{R}}} F_k^-$ corresponds to a reflection of particles at the transport–diffusion interface with attenuation of statistical weight by the factor $(1-\zeta)$. Consequently, the corresponding loss of weight is deposited in the right diffusion cell. The term $\frac{\zeta\alpha_T}{4}\Theta_T^{\mathrm{R}}$ multiplied by the time-step Δt corresponds to an energy emission from the diffusion cell into the Monte-Carlo region. Of course, only particles with energy group between $k_{\mathrm{L}}+1$ and k_{R} are affected. This will change the structure of linear system (19).

We must distinguish between symbolic particles whose initial weight is proportional to Θ_M and which corresponds to the volume source term in (7) and symbolic particles whose initial weight is proportional to Θ_T and which corresponds to the emission of energy at transport–diffusion interfaces in (24). On the other hand, we must also distinguish between energy deposited at transport–diffusion interfaces and energy deposited through absorption in Monte-Carlo cells. In Monte-Carlo cells, energy deposit (17) becomes

$$\int_t^{t+\Delta t} \mathrm{d}s \sum_{k=k^{\mathrm{c}}+1}^{K} \sigma_k \int I_k(\vec{\Omega})\,\mathrm{d}\vec{\Omega} = S^{\mathrm{M}} + \mathscr{M}_{\mathrm{M}}^{\mathrm{M}}\Theta_M + \mathscr{M}_{\mathrm{T}}^{\mathrm{M}}\Theta_T,$$

and at transport–diffusion interfaces, energy deposit writes as

$$\int_t^{t+\Delta t} \mathrm{d}s \sum_{k=k^{\mathrm{L}}+1}^{k_{\mathrm{R}}} \mathrm{div}\left(\frac{b_k}{3\sigma_k}\nabla\Theta_T\right) = S^{\mathrm{T}} + \mathscr{M}_{\mathrm{M}}^{\mathrm{T}}\Theta_M + \mathscr{M}_{\mathrm{T}}^{\mathrm{T}}\Theta_T,$$

where $\mathscr{M}_{\mathrm{M}}^{\mathrm{M}}$, $\mathscr{M}_{\mathrm{T}}^{\mathrm{M}}$, $\mathscr{M}_{\mathrm{M}}^{\mathrm{T}}$ and $\mathscr{M}_{\mathrm{T}}^{\mathrm{T}}$ are Monte-Carlo matrices. Finally, the space discretization of diffusion operator for the thermalization temperature Θ_T is simply derived from (22):

$$\Delta t \sum_{k=1}^{k_{\mathrm{L}}} \mathrm{div}\left(\frac{b_k}{3\sigma_k}\nabla\Theta_T\right) = \mathscr{D}\Theta_T.$$

We rewrite now the final linear system (19) in the general case

$$\mathscr{A}\begin{bmatrix}\Theta_T\\ \Theta_M\end{bmatrix} = \begin{bmatrix}\alpha\Theta_T^0 + S^{\mathrm{T}}\\ \Theta_M^0 + S^{\mathrm{M}}\end{bmatrix}, \tag{25}$$

where the Monte-Carlo matrix $\mathscr{A}$ is just

$$\mathscr{A} = \begin{bmatrix}\left(\alpha + \Delta t\sigma^{\mathrm{E}} + \Delta t\frac{\zeta\alpha_T}{4}\right)I_d - \mathscr{D} - \mathscr{M}_{\mathrm{T}}^{\mathrm{T}} & -\Delta t\sigma^{\mathrm{E}}I_d - \mathscr{M}_{\mathrm{M}}^{\mathrm{T}}\\ -\Delta t\sigma^{\mathrm{E}}I_d - \mathscr{M}_{\mathrm{T}}^{\mathrm{M}} & (1+\Delta t\sigma^{\mathrm{T}})I_d - \mathscr{M}_{\mathrm{M}}^{\mathrm{M}}\end{bmatrix}. \tag{26}$$

4. Properties of the Monte-Carlo matrix

In this section, we shall prove that the $2n \times 2n$ matrix $\mathscr{A}$ given by (26) is strictly diagonally dominant and thus invertible.

For this purpose, we prove that the two following $n \times n$ matrices obtained by adding extra-diagonal sub-matrices of $\mathscr{A}$ to the diagonal sub-matrices are themselves diagonally dominant:

$$\begin{aligned}\mathscr{A}^{\mathrm{T}} &= \left(\alpha + \Delta t\sigma^{\mathrm{E}} + \Delta t\frac{\zeta\alpha_\Gamma}{4}\right)I_d - \mathscr{D} - \mathscr{M}_{\mathrm{T}}^{\mathrm{T}} - \Delta t\sigma^{\mathrm{E}}I_d - \mathscr{M}_{\mathrm{T}}^{\mathrm{M}} \\ &= \left(\alpha + \Delta t\frac{\zeta\alpha_\Gamma}{4}\right)I_d - \mathscr{D} - \mathscr{M}_{\mathrm{T}}^{\mathrm{T}} - \mathscr{M}_{\mathrm{T}}^{\mathrm{M}}, \\ \mathscr{A}^{\mathrm{M}} &= \left(1 + \Delta t\sigma^{\mathrm{T}}\right)I_d - \mathscr{M}_{\mathrm{M}}^{\mathrm{M}} - \Delta t\sigma^{\mathrm{E}}I_d - \mathscr{M}_{\mathrm{M}}^{\mathrm{T}} \\ &= \left(1 + \Delta t(\sigma^{\mathrm{T}} - \sigma^{\mathrm{E}})\right)I_d - \mathscr{M}_{\mathrm{M}}^{\mathrm{M}} - \mathscr{M}_{\mathrm{M}}^{\mathrm{T}}.\end{aligned} \tag{27}$$

Let us first consider $\mathscr{A}^M$. $\mathscr{M}_{\mathrm{M}}^{\mathrm{M}}$ is the Monte-Carlo matrix which represents the energy deposited through absorption of symbolic Monte-Carlo particles sampling the volume emission term and $\mathscr{M}_{\mathrm{M}}^{\mathrm{T}}$ is the Monte-Carlo matrix which represents the energy deposited through attenuation at transport–diffusion interfaces of the same population of particles. On the other hand $\Delta t(\sigma^{\mathrm{T}} - \sigma^{\mathrm{E}})I_d$ represents the volume emission term. So on column j, the matrix term $(\mathscr{M}_{\mathrm{M}}^{\mathrm{M}} + \mathscr{M}_{\mathrm{M}}^{\mathrm{T}})_{i,j}$ is the energy absorbed on cell j from symbolic particles coming from cell i and $\Delta t(\sigma^{\mathrm{T}} - \sigma^{\mathrm{E}})$ is just the energy of these particles. As absorbed energy cannot be greater than emitted energy we necessarily have

$$\sum_j (\mathscr{M}_{\mathrm{M}}^{\mathrm{M}} + \mathscr{M}_{\mathrm{M}}^{\mathrm{T}})_{i,j} \leqslant \Delta t(\sigma^{\mathrm{T}} - \sigma^{\mathrm{E}}),$$

which implies that $\mathscr{A}^{\mathrm{M}}$ is strictly diagonally dominant.

The argument is similar for matrix $\mathscr{A}^{\mathrm{T}}$. $\mathscr{M}_{\mathrm{T}}^{\mathrm{M}}$ and $\mathscr{M}_{\mathrm{T}}^{\mathrm{T}}$ represents energy deposited, respectively, through absorption in Monte-Carlo cells and attenuation at transport–diffusion interfaces. The symbolic particles are now those which have been emitted at transport–diffusion interfaces and the total energy emitted is just $\Delta t(\zeta\alpha_\Gamma/4)$.

Hence $\Delta t(\zeta\alpha_\Gamma/4)I_d - \mathscr{M}_{\mathrm{T}}^{\mathrm{M}} - \mathscr{M}_{\mathrm{T}}^{\mathrm{T}}$ is diagonally dominant. $-\mathscr{D}$ is also diagonally dominant (it is a tridiagonal matrix coming from the spatial discretization of a diffusion operator). Taking into account the term coming from the time derivative αI_d, we conclude that $\mathscr{A}^{\mathrm{T}}$ is strictly diagonally dominant.

We have seen that Monte-Carlo matrix $\mathscr{A}$ is strictly diagonally dominant: this implies that it is invertible.

We end this section by studying the behavior of $\mathscr{A}$ in the two limiting cases where mean free path is very small or very large. If the spectral cut-off is adequately chosen it means that either $k^{\mathrm{c}}(x,t) \equiv 0$ or $k^{\mathrm{c}}(x,t) \equiv K$. In the first case, we get:

$$\mathscr{A}_{\sigma\to\infty} \sim \begin{bmatrix} (\alpha + \Delta t\sigma^{\mathrm{T}})I_d - \mathscr{D} & -\Delta t\sigma^{\mathrm{T}}I_d \\ -\Delta t\sigma^{\mathrm{T}}I_d & (1 + \Delta t\sigma^{\mathrm{T}})I_d \end{bmatrix}$$

and we recover a grey diffusion problem. In the second case, we obtain

$$\mathscr{A}_{\sigma\to 0} \sim \begin{bmatrix} 0 & 0 \\ 0 & (1 + \Delta t\sigma^{\mathrm{T}})I_d - \mathscr{M}_{\mathrm{M}}^{\mathrm{M}} \end{bmatrix},$$

that is, we recover standard SMC matrix (see [6]).

5. Numerical results

In this section, we show the behavior of the model on a benchmark, proposed by Olson and Su [8].

It consists in solving the radiative transfer equations in a one-dimensional infinite and homogeneous medium. The number of frequency groups is set to two and the corresponding opacities σ_1 and σ_2 are constant. A frequency uniformly distributed radiative source term is localized near the origin. Moreover,

since the material specific heat is assumed to be proportional to the cube of the material temperature, the problem is linear and it is possible to compute the exact solution by performing a Laplace transform in time and a Fourier transform in space.

The system writes as

$$\partial_t I_k + \vec{\Omega}\cdot\nabla I_k + \sigma_k\left(I_k - \frac{b_k}{4\pi}\Theta_M\right) = \frac{b_k}{4\pi}\mathbb{I}(|x|<0.5)\mathbb{I}(t<10)$$

$$\partial_t \Theta_M + \sum_{k=1}^{2}\int \sigma_k\left(\frac{b_k}{4\pi}\Theta_M - I_k\right)\mathrm{d}\vec{\Omega} = 0, \quad k=1,2,$$

where $\mathbb{I}$ denotes the indicatrix function. The reduced Planck's function does not depend on the temperature $b_1 = b_2 = 1/2$ and we have $\sigma_1 = 200/101$, $\sigma_2 = 2/101$ so that the arithmetic mean of opacities $b_1\sigma_1 + b_2\sigma_2$ is equal to 1. At last, initial conditions is $I_k(x,\vec{\Omega},0) = \Theta_M(x,0) = 0$ and boundary condition is $\lim_{x\mapsto\pm\infty} I_k(x,\vec{\Omega},t) = 0$ for all time t.

The source term is localized for $|x| < 0.5$ and $0 \leqslant t < 10$ so we discretize the problem using a regular mesh of 3000 cells over the space interval $(0,30)$ with reflecting boundary condition on $x = 0$ and zero incoming flux at $x = 30$: this reproduces the exact boundary condition since no photon reaches the right boundary at $t = 10$, the end time of the simulation.

The size of each cell (0.01) is smaller than the mean free path for each frequency ($101/200$ and $101/2$) which allows us to use the transport description for both frequencies. The initial null temperature is approximated by a temperature of 10^{-4}. The initial time-step is 3×10^{-4}, the maximum time-step is 3×10^{-2}.

The results in [8] are given in terms of

$$U_1(x,t) = \int I_1(x,\vec{\Omega},t)\,\mathrm{d}\vec{\Omega}, \quad U_2(x,t) = \int I_2(x,\vec{\Omega},t)\,\mathrm{d}\vec{\Omega}.$$

We denote UTRANS $= U_1 + U_2$, VTRANS $= \Theta_M$, U1TRAN $= U_1$ and U2TRAN $= U_2$ the solutions given by Fourier–Laplace transforms and UCALC $= U_1 + U_2$, VCALC $= \Theta_M$, U1CALC $= U_1$ and U2CALC $= U_2$ the solutions given by various numerical experiments. We present the results of three such computations (all figures represent energies as a function of space in the x-axis):

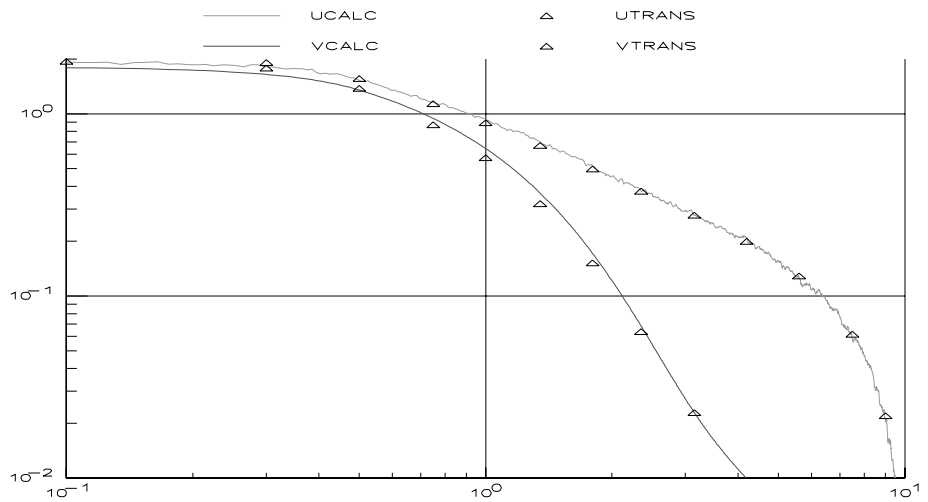

Fig. 3. Case 1: exact and hybrid transport (lowest group in diffusion) solution at $t = 10$.

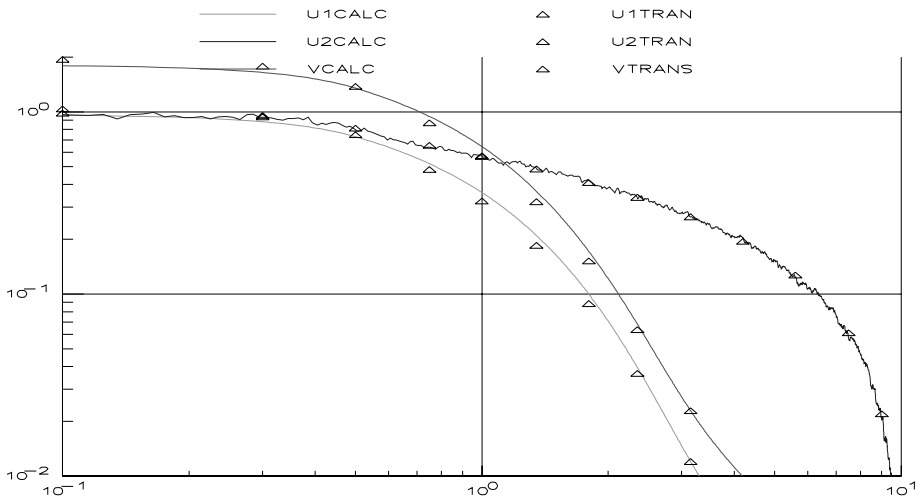

Fig. 4. Case 1: exact and hybrid transport (lowest group in diffusion) solution at $t = 10$.

Case 1. The spectral cut-off k_c is set to 1, so the first frequency group is solved in the diffusion approximation and the second in the transport description.

The difference between U1CALC and U1TRAN (Fig. 4) near the origin suggests that the diffusion approximation for the first group is not valid: U1CALC is too small near 0 and too high after 0.5. Due to the strong coupling between the matter and the photons for the frequency 1, the material energy VCALC has the same behavior (Fig. 3). In contrast, the result for the second group is quite satisfactory.

The reason of this discrepancy is that the size of the source is of the same order (0.5) as the mean free path in the first the frequency group (101/200). It is well known that in a boundary layer of some mean free paths near the source, the diffusion approximation is no longer valid [7].

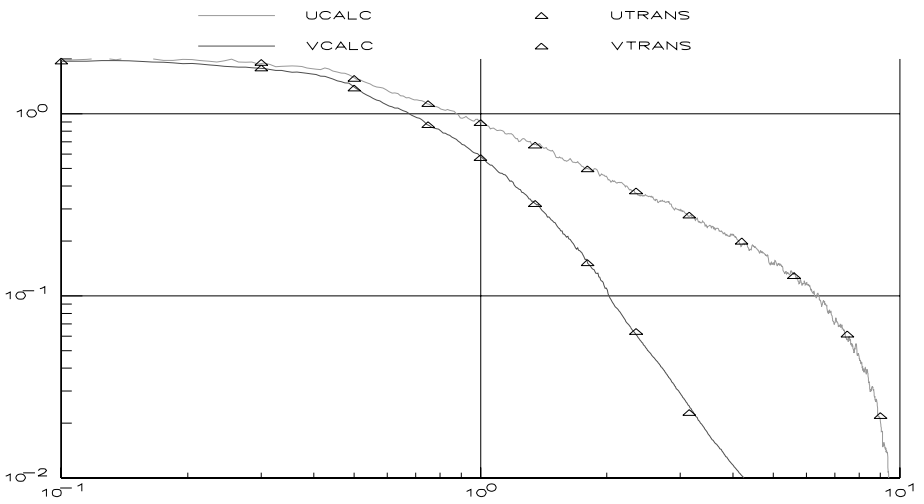

Fig. 5. Case 2: exact and hybrid transport (lowest group in diffusion for $x > 2$) solution at $t = 10$.

Case 2. To improve the treatment of the first frequency group, in this second calculation, it is only partially treated in the diffusion approximation: the spectral cut-off k_c is now set to 0 for $x < 2$ and to 1 for $x > 2$ so the first frequency group is solved in the transport description for $x < 2$ and in the diffusion approximation for $x > 2$. The second frequency group is still described by the transport equation.

We see (Figs. 5 and 6) that in this case the agreement between the calculated and the exact solutions is very satisfactory (see Fig. 7).

Case 3. In this third calculation, we solve the full transport equations for both frequencies which is feasible because the mean free paths for the both frequencies are smaller than the cell size. This is done by setting the spectral cut-off to 0 everywhere. The agreement between the calculated and the exact solutions is also good but we notice oscillations in the material energy VCALC (Fig. 8) which are clearly due to the Monte-Carlo treatment of the first frequency group.

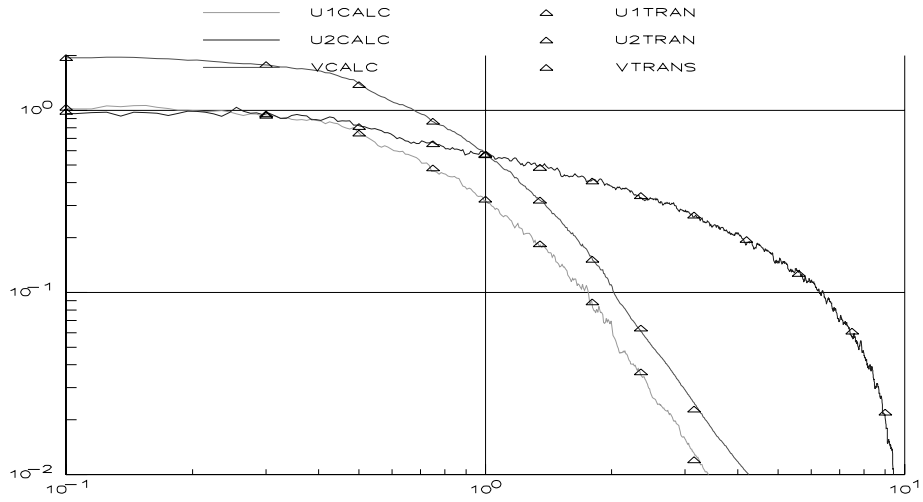

Fig. 6. Case 2: exact and hybrid transport (lowest group in diffusion for $x > 2$) solution at $t = 10$.

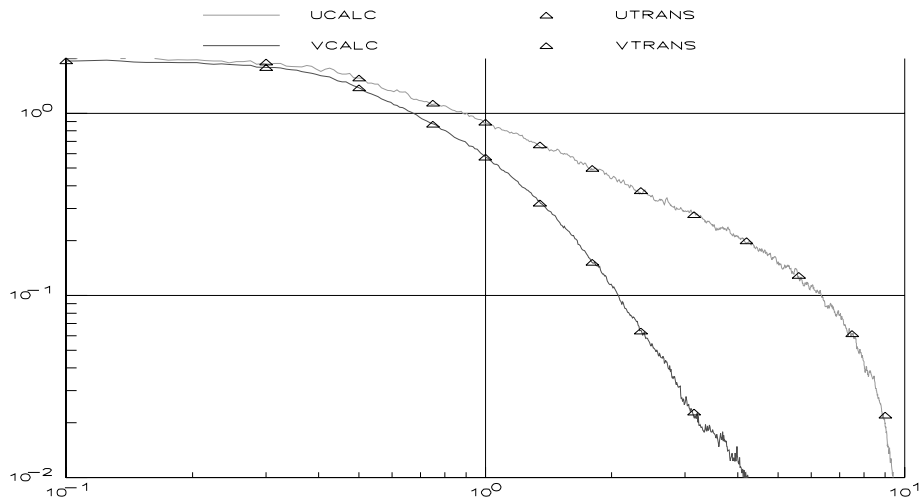

Fig. 7. Case 3: exact and full transport solution at $t = 10$.

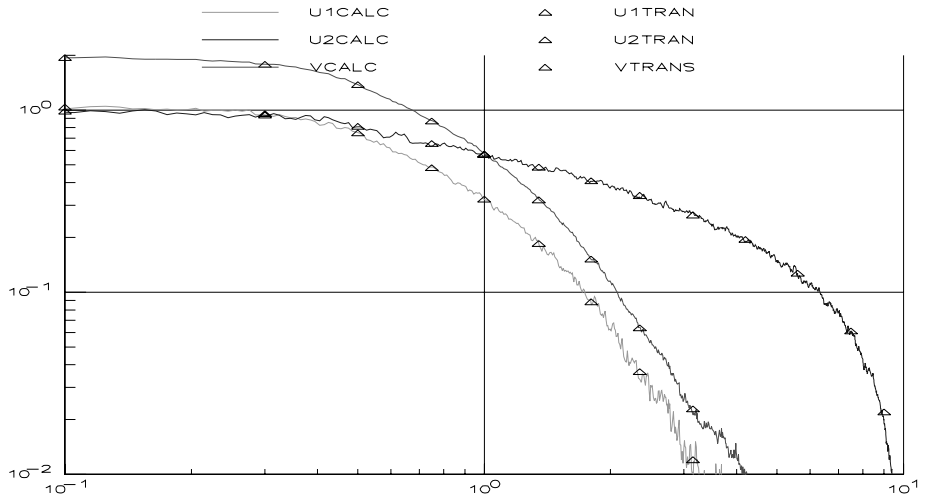

Fig. 8. Case 3: exact and full transport solution at $t = 10$.

So provided that the spectral cut-off is adequately chosen, the method gives correct results. We can now discuss its precision: it will be done in next section.

6. Computational issues

A complete analysis of the benefits of this method compared to IMC method is beyond the scope of this paper and should be strongly dependent on the application. We will however discuss the accuracy of the method on previous benchmark. We have computed a figure of merit for Hybrid SMC (case 2) and Full SMC (case 3) methods. The figure of merit at time t and position x is defined by:

$$\mathrm{FOM}(x,t) = \langle (\Theta_M(x,t) - \langle \Theta_M(x,t) \rangle)^2 \rangle \times \mathrm{CPU}_{\mathrm{cost}},$$

where $\langle \cdot \rangle$ denotes average over many computations. Actually, we only used an approximation of this quantity by computing for only one realization

$$\overline{\mathrm{FOM}}(x,t) = \frac{1}{2\epsilon} \int_{x-\epsilon}^{x+\epsilon} (\Theta_M(y,t) - \overline{\Theta_M}(y,t))^2 \,\mathrm{d}y \times \mathrm{CPU}_{\mathrm{cost}},$$

where ϵ is a small parameter and $\overline{\Theta_M}(y,t)$ is a linear approximation of $\Theta_M(y,t)$ on $(x-\epsilon, x+\epsilon)$. By changing the number of Monte-Carlo particles emitted at each time-step, we have computed the figure of merit at time $t = 10$ for various positions x (ϵ was taken equal to 0.07):

- For a given number of emitted particles, the $\mathrm{CPU}_{\mathrm{cost}}$ are comparable for Hybrid SMC (case 2) and Full SMC: Hybrid SMC is approximatively 15% more expensive than Full SMC because of the extra Monte-Carlo events at the boundary between transport and diffusion regions.
- When $x \leqslant 2$, the full transport equations are solved for both frequencies in SMC and Hybrid SMC. For a given number of emitted particles the variance is comparable so the figure of merit of Full SMC is slightly better than that of Hybrid SMC (Fig. 9).
- When $x \geqslant 2$, the lowest group is treated in the diffusion approximation in Hybrid SMC. There are several orders of magnitude between the variance of both methods (Fig. 10).

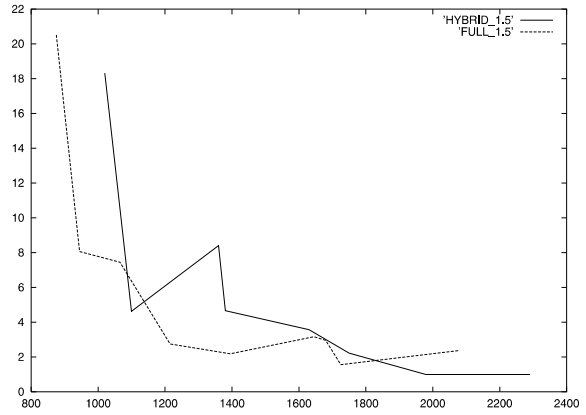

Fig. 9. Variance (arbitrary unit) as a function of CPU_{cost} (in second) at $x = 1.5$, $t = 10$ for Full SMC and Hybrid SMC.

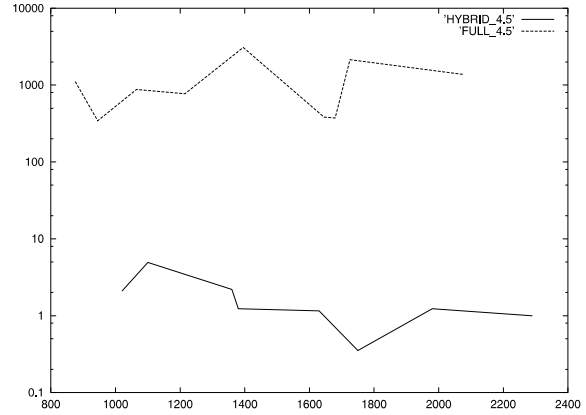

Fig. 10. Variance (arbitrary unit) as a function of CPU_{cost} (in second) at $x = 4.5$, $t = 10$ for Full SMC and Hybrid SMC.

Hence, in this case, Hybrid SMC is efficient for reducing random noise far from the location of the source term.

In the general case, the situation is of course completely different, according to the optical thickness of the medium. In an optically thin medium, we recover Full SMC and the method behave similarly (the extra cost for Hybrid SMC being small). In an optically thick medium, we recover the diffusion limit, i.e., we only solve a diffusion equation with finite differences method. In this case Full SMC behaves poorly [3] so Hybrid SMC is a simple way to improve SMC for this kind of problems.

For purpose of comparison with IMC method, we should compare the computational cost of tracking symbolic particles and inverting the linear system with the computational cost of Fleck's collision and random walk events: it will depend on time-step, opacity and mesh size. If the medium is optically thin, the methods behave similarly; if the medium is optically thick Hybrid SMC is more efficient because it is equivalent to diffusion approximation solved by finite differences instead of random walk. In the intermediate case, we cannot conclude in full generality: there may be a need for specific benchmark.

One of the questions which arise about SMC methods (Full and Hybrid) is the storage of Monte-Carlo matrix and the cost of the inversion of the linear system. First, we point out the fact that there is no extra computational cost due to the multi-group discretization in Hybrid SMC because we took a grey

approximation for the low energy groups. From a practical point of view, inverting the linear system requires an iterative solver for non-symmetric matrices when the number of cells becomes large. One of the drawback of the method is that $\mathscr{A}$ can possibly become a non-sparse matrix. It is easy to see that, for a given column j the number of non-zero terms is equal to the number of cells visited by particles issued from cell j which is bounded by $\Delta t/h$ or rather $c(\Delta t/h)$ with c the speed of light (remember that we had previously set c to one). In radiation hydrodynamics computations, the time-step is usually constrained by a CFL condition which writes as $c_s(\Delta t/h) \leqslant 1$ where c_s is the speed of sound waves. So we see that the number of non-zero terms is only bounded by c/c_s which is very large. However, we notice that, when opacity is large, particles are absorbed very close to their originating cell so that the number of cells is small and, when opacity is small, particles can travel very far without being absorbed so that the number of cells may becomes large but on the other hand the whole matrix $\mathscr{A}$ becomes strongly diagonally dominant so there is no problem with the inversion of the linear system (problems arise rather from memory storage). We will not argue anymore on this aspect but we have to keep in mind that this can be an issue for the method especially in multidimensional problems.

7. Conclusions

In this paper we have described a new hybrid method to solve the radiative transfer equations. We introduced the notion of spectral cut-off which enables to split the spectrum into two parts, the lower part which corresponds to optically thick frequencies is treated in the diffusion approximation whereas the higher part which corresponds to optically thin frequencies is described by the full transport equation. We have seen that Symbolic Monte-Carlo is particularly well adapted to such a modeling. We have also provided numerical tests which show the relevance of this approach on frequency-dependent problems. This aspect was rarely tackled in previous works.

One of the interest of the method is that the diffusion limit is automatically obtained if we are able to set a criterion to say when (in time) and where (in space and frequency) the transport equation can be approximated by the diffusion model. This can be an issue if a local criterion is not adequate. Such a criterion should be based on a comparison between the spectral mean free path and the gradient length of some quantity like the temperature. One should also take into account the time of absorption for this frequency compared to some time scale. In practice, a criterion which takes into account the optical depth of the cell should always be adequate because it is possible to track Monte-Carlo particles with a good accuracy if the cells are optically thin. However this criterion could overestimate the need for a transport description and lead to too costly simulations. The determination of a good criterion in the general case is currently under work.

References

[1] M. Adams, Nucl. Sci. Eng. 137 (2001) 298.
[2] E.D. Brooks III, J. Comput. Phys. 83 (1989) 433.
[3] J.-F. Clouët, G. Samba, in preparation.
[4] J.A. Fleck, J.D. Cummings, J. Comput. Phys. 8 (1971) 313.
[5] N.A. Gentile, J. Comput. Phys. 172 (2001) 543.
[6] T.N'. Kaoua, J. Sci. Stat. Comput. 12 (1991) 505.
[7] E.W. Larsen, G.C. Pomraning, V.C. Badham, J. Quant. Spectrosc. Radiat. Transfer 29 (1983) 285.
[8] G. Olson, B. Su, J. Quant. Spectrosc. Radiat. Transfer 62 (1999) 279.
[9] G.C. Pomraning, The Equations of Radiation Hydrodynamics, Pergamon, Oxford, 1973.
[10] G.C. Pomraning, G.M. Foglesong, J. Comput. Phys. 32 (1979) 420.